We are IntechOpen,
the world's leading publisher of
Open Access books
Built by scientists, for scientists

4,800

Open access books available

122,000

International authors and editors

135M

Downloads

154

Countries delivered to

Our authors are among the

TOP 1%

most cited scientists

12.2%

Contributors from top 500 universities

CLARIVATE ANALYTICS
BOOK CITATION INDEX
INDEXED

WEB OF SCIENCE™

Selection of our books indexed in the Book Citation Index
in Web of Science™ Core Collection (BKCI)

Interested in publishing with us?
Contact book.department@intechopen.com

Numbers displayed above are based on latest data collected.
For more information visit www.intechopen.com

Chapter

Mathematical Modeling and Well-Posedness of Three-Dimensional Shell in Disorders of Human Vascular System

Vishakha Jadaun and Nitin Raja Singh

Abstract

Aortic dissection is the most common aortic emergency requiring surgical intervention. Whether the elective endovascular repair of abdominal aortic aneurysm reduces long-term morbidity and mortality, as compared with traditional open repair, remains uncertain. The foundation of shell element based on the Reissner-Mindlin kinematics assumption is widely applicable, but this cannot model applications of shell surface stresses as needed in analysis of shell in human vascular system. The analysis is designed to assess progression of initial lesion in aortic dissection. Using general shell element analysis and tensor calculus, a higher order differential geometry-based model is proposed. Since the shell is thin, a variational formulation for initial lesion is proposed. The variational formulation for initial lesion is well posed. The weak convergence of the solution to initial lesion model is mathematically substantiated. Asymptotic analysis shows that initial lesion is membrane-dominated and bending-dominated when pure bending is inhibited and noninhibited, respectively. At least two observations are to be noted. First, the mathematical analysis of the initial lesion model is distinct from classical shell models. Second, the asymptotic analysis of the initial lesion model is based on degenerating three-dimensional continuum to bending strains in order to assess initial lesion behavior.

Keywords: aortic dissection, higher order kinematical assumptions, initial lesion model, variational formulation, asymptotic analysis

1. Introduction

The shell structure is generally a three-dimensional structure that is elongated in two directions and thinned out in other direction. The shell structures in nature are profusely impressive such as seashells and eggshells. In various industries including aeronautics, naval architecture, and automotive engineering milieu, many engineering designs are analyzed to design shells as thin as possible and optimize the amount of material [1]. Human anatomy develops cyst-related diseases with progressive severity. These disease states involve single to multiple cyst formations

in distinct organ systems including the lung, liver, kidney, brain, bone etc. Pathophysiologically, these cysts emanate from either the underlying genetic anomaly or infections such as helminths and mycobacterial, among others. Interestingly, these cysts can be modeled as shells, albeit in higher dimensions.

Different approaches have been formulated for shell elements discretization. One of the approaches [2] evaluated the shell behavior as the superimposition of membrane bending action as well as plate bending action. The discrete construction of shell elements requires a combination of plane stress matrices as well as plate bending stiffness matrices. However, the resultant shell elements are less accurate since curvature effects are not duly incorporated and the membrane behavior and plate bending behavior are coupled at nodal points only. Another approach [3] is based on variational formulation and perusing relevant shell theory wherein a specific shell theory is constituted of higher-order derivatives and required concomitant nodal point variables beyond the conventional nodal point rotations and displacements. Such an approach is applicable and relevant to certain shell geometries and associated pertinent analysis conditions. Thus, it is difficult to model more complex shell structures. Yet another approach [4] is aimed for very general formulation related to three-dimensional continuum degeneration. In this approach, the mid-surface of the shell element that belongs to the three-dimensional continuum is clearly defined and identified. The first assumption is that the fibers are straight and normal to mid-surface prior to the deformation which continues to remain straight during the course of deformation. The second assumption is that the stress normal to the shell mid-surface is zero throughout the shell motion [5, 6]. The shell models based on the aforementioned kinematical assumptions can be interpreted as a truncation of the expansion of displacements in different directions across the thickness of the shell structure. It is to be noted that such truncated expansion contains terms up to degree one and degree zero for the tangential displacements and transverse displacements, respectively. The physiological and pathological states in the human body undergo dynamic transformations. In cardiovascular dynamics, the interaction of blood to the internal vessel lining is associated with large through-the-thickness displacement of local vessel wall surface owing to distension by propulsion of blood and elastic recoil thereafter. Thus, the aforementioned assumptions might not be applicable to shells in human anatomy. In order to make better estimate, higher-order kinematical assumptions are effective. Yet the detailed analysis of biological shell structures frequently presents challenging problems. One of the difficulties is that the shell structure resists applied loads largely along its curvature such that, in case, curvature is changed and the load bearing capacity of shell is transformed. Therefore, analysis of boundary conditions of a shell structure plays a vital role in shell behavior and its response to stress.

The aorta is the largest diameter blood vessel, emerging from the left ventricle to supply oxygenated blood to the human body. Whenever nonlinear degeneration of the tunica media (middle layer of the vessel wall) occurs, the aorta undergoes dynamic dilatation and marginal elongation. Generally, this degeneration is caused by genetic anomaly and prolonged untreated hypertension in young and senile patients, respectively. It is termed as *aortic aneurysm* [7]. Whenever there is structural discontinuity in nonconformal internal vessel wall, the blood surges through the tear causing the inner and middle layers of the aorta to separate. It is termed as *aortic dissection* (AD) [8]. AD is a life-threatening condition [9]. If the blood-filled channel ruptures through the outside aortic wall, AD is often fatal [10]. It is the most common aortic emergency requiring surgical intervention. AD is classified according to the regional involvement of the segment of the aorta with the Stanford type A dissection and the Stanford type B dissection involving the ascending aorta and occurring distal to the left subclavian artery, respectively. According to the international guidelines on clinical therapeutics, uncomplicated type B dissection should receive optimal medical treatment (OMT). However, in spite of adequate

hypertension-related treatment, patients may develop a significant aortic enlarge-
ment that necessitates operative intervention. These chronic patients will benefit in
the long-term from prophylactic intervention.

Currently, there is no consensus on the management of uncomplicated type B
dissection that may be liable for rapid progression. Thus, seeking multiple high-risk
attributes/features responsible for rapid progression might help to decide when to
treat and how to treat. There is a subgroup of patients who progress very rapidly
to terminal dilatation liable for rupture and torrential bleed leading to death.
Offering early transthoracic endovascular repair to this subgroup seems to be a
life-saving proposition. Finding these patients is a challenge. It is not known that
a patient at risk for catastrophic events is following a personal trajectory of
disease progression. It is also not known that a threshold for disease progression
that can predict a high risk of mortality for a specific patient. By modeling the
initial lesion of AD, we can potentially avoid rupture by crossing over to
transthoracic endovascular repair at a time that minimizes procedural risks. On
asymptotic analysis, we evaluate the point of follow-up; we lose the ability to
achieve the same desirable aortic remodeling observed with transthoracic
endovascular repair in the more acute setting. Therefore, reliable predictors are
needed in the early stage of disease. It aids identification of patients at risk of
aortic enlargement.

In early stages of AD, subintimal intramural hemorrhage occurs due to tunica
media degeneration. In certain situations, when strains are known on a plane, the
low degree of expansion of the transverse displacement is to be recovered. It is to be
noted that by dispensing away the assumption of plane stress, an arbitrary three-
dimensional material law is applicable in three-dimensional formulation of contin-
uum mechanics. The objective of this chapter is to identify higher-order shell model
for initial-stage primary tunica intimal lesion of AD by the general shell element
approach and to perform mathematical analysis.

This chapter is organized in the following manner. In Section 2, we give certain
definitions, conventions, and notations relevant to the shell geometry and its
corresponding deformation. Next in Section 3, we derive initial lesions of AD as the
higher-order shell model perusing general shell analysis approach. Then in Section
4, we do mathematical analyses of the initial lesions described in the previous
section. In Section 5, we assess asymptotic behavior of the model. Finally, in Section
6, we present our conclusions regarding mathematical modeling of shells in human
vascular tissues and future scope.

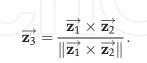## 2. Conventions and notations in higher-order shell geometry

We are interested in modeling early stages of AD; the initial subintimal intra-
mural hemorrhage caused by tunica media degeneration undergoes solidification
due to clot formation. Thus, this initial lesion closely follows the principles of
continuum mechanics. We consider the initial lesion as a solid medium. It is geo-
metrically defined by a mid-surface immersed in the human vascular compartment
ϵ (dimensionless thickness parameter) and a parameter representing the thickness
of the medium around this surface.

In order to understand the initial lesion of AD, we model the initial lesion using
general shell element theory. A shell is defined as a collection of charts. Let us
consider the mid-surface of a shell as a collection of two-dimensional charts. These
charts are smooth ono-one maps from domains of $\mathbb{R}^2$ into Euclidean (physical)
space $\mathscr{E}$. We consider an initial lesion with a mid-surface $\mathscr{S}$ defined by a two-
dimensional chart $\vec{\varphi}$, which is a one-one map from the closure of a bounded open

subset of $\mathbb{R}^2$, denoted by ω, into $\mathscr{E}$, hence $\mathcal{S} = \vec{\varphi}\left(\vec{\omega}\right)$. At each point of the mid-surface, the vector $\vec{\mathbf{z}}_\alpha$ is assumed as partial derivative of $\vec{\varphi}$ with respect to ξ^α such that

$$\vec{\mathbf{z}}_\alpha = \frac{\partial \varphi(\xi_1, \xi_2)}{\partial \xi^\alpha}. \tag{1}$$

These vectors are linearly independent from each other, so that they form a basis of the plane tangent to the mid-surface at this point. The unit normal vector is given by

$$\vec{\mathbf{z}_3} = \frac{\vec{\mathbf{z}_1} \times \vec{\mathbf{z}_2}}{\|\vec{\mathbf{z}_1} \times \vec{\mathbf{z}_2}\|}.$$

Definition 1. (Geometric definition of initial lesion). *An initial lesion is a solid medium whose domain Ω can be defined by a mid-surface whose map is given by*

$$\varphi : \omega \subseteq \mathbb{R}^2 \to \mathbb{R}^3, s.t. \; \varphi\left(\xi^1, \xi^2\right) = \left(\xi^1, \xi^2, \xi^3\right) \in \mathbb{R}^3 \tag{2}$$

The three-dimensional medium corresponding to the initial lesion is then defined by three-dimensional chart given by

$$\varphi\left(\xi^1, \xi^2, \xi^3\right) = \varphi\left(\xi^1, \xi^2\right) + \xi^3 \vec{\mathbf{z}}_3\left(\xi^1, \xi^2\right), \tag{3}$$

where $\left(\xi^1, \xi^2, \xi^3\right) \in \Omega = \left\{ \left(\xi^1, \xi^2, \xi^3\right) \in \mathbb{R}^3 | \left(\xi^1, \xi^2\right) \in \omega, \xi^3 \in \left(-\frac{t\left(\xi^1, \xi^2\right)}{2}, \frac{t\left(\xi^1, \xi^2\right)}{2} \right) \right\}$ and $t\left(\xi^1, \xi^2\right)$ is the thickness of the initial lesion element at $\left(\xi^1, \xi^2\right)$.

In Eq. (1), we have defined tangent vector to a point on the mid-surface of the initial lesion (2) which lies in the region of the Euclidean space. Since we are interested in higher-order parameterization of the initial lesion of AD, the three-dimensional chart (3) of this lesion can be very helpful. Thus, transition from the Euclidean space to curvilinear coordinate system will aid to model higher-order initial lesion. It is relevant to grasp few basic notions of surface differential geometry.

2.1 Definitions related to surface differential geometry

Definition 2. (Covariant vector). *Let $r(z)$ be a position vector; the differentiation of $r(z)$ with respect to each of the coordinate is called covariant basis:*

$$z_i = \frac{\partial r(z)}{\partial z^i} \tag{4}$$

If Eq. (4) defines three vectors $\mathbf{z}_1$, $\mathbf{z}_2$, and $\mathbf{z}_3$

$$\mathbf{z}_1 = \frac{\partial \, r(z^1, z^2, z^3)}{\partial z^1}, \quad \mathbf{z}_2 = \frac{\partial \, r(z^1, z^2, z^3)}{\partial z^2}, \quad \mathbf{z}_3 = \frac{\partial \, r(z^1, z^2, z^3)}{\partial z^3}. \tag{5}$$

Let $\mathbf{V}$ be a vector in $\mathbb{R}^3$, and then its expansion n terms of basis is

$$\mathbf{V} = V^i \mathbf{z}_i = V^1 \mathbf{z}_1 + V^2 \mathbf{z}_2 + V^3 \mathbf{z}_3 \tag{6}$$

The values V^i are called *contravariant components* of vector $\mathbf{V}$.

Interestingly, covariant basis is useful in the modeling of higher-order initial lesions in human vascular system given by

$$
\begin{cases}
\vec{g}_i = \dfrac{\partial \varphi}{\partial \xi^i} = z_i + \xi^3 \, \mathbf{z}_{\overrightarrow{3,i}} = \mathbf{z}_{\vec{i}} - \xi^3 \, b_i^k \cdot \overrightarrow{\mathbf{z}_k}, \quad \text{where} \quad \mathbf{z}_{\overrightarrow{3,i}} = \dfrac{\partial \mathbf{z}_{\vec{3}}}{\partial \xi^i}, \\[2mm]
\vec{g}_i = \left(\delta_i^k - \xi^3 \, b_i^k \right) \overrightarrow{\mathbf{z}_k}, \\[2mm]
\vec{g}_3 = \dfrac{\partial \varphi}{\partial \xi^3} = \overrightarrow{\mathbf{z}_3}.
\end{cases}
\tag{7}
$$

Definition 3. (Covariant metric tensor). *The covariant metric tensor is the pairwise dot product of the covariant basis vectors:*

$$
z_{ij} = z_i . z_j =
\begin{bmatrix}
z_1.z_1 & z_1.z_2 & z_1.z_3 \\
z_2.z_1 & z_2.z_2 & z_2.z_3 \\
z_3.z_1 & z_3.z_2 & z_3.z_3
\end{bmatrix},
\tag{8}
$$

where z_i is in $\mathbb{R}^3$.

Suppose two vectors $\mathbf{A}$ and $\mathbf{B}$ are located at the same point and their components are A^i and B^i, then the dot product $\mathbf{A}.\mathbf{B}$ is given by

$$
\mathbf{A}.\mathbf{B} = A^i \mathbf{z}_i . B^j \mathbf{z}_j = \left(\mathbf{z}_i \cdot \mathbf{z}_j \right) A^i \cdot B^j = z_{ij} A^i B^j.
\tag{9}
$$

The length of a vector $\mathbf{B}$ can be expressed in terms of covariant metric tensor as

$$
|\mathbf{B}| = \sqrt{z_{ij} B^i B^j}
\tag{10}
$$

Interestingly, covariant tensors are useful in modeling of higher-order initial lesions in human vascular system given by

$$
1. g_{ij} = \vec{g}_i \cdot \vec{g}_j = \mathbf{z}_{ij} - 2\xi^3 b_{ij} + \left(\xi^3 \right)^2 c_{ij}
$$

$$
2. g_{i3} = \vec{g}_i \cdot \vec{g}_3 = 0
$$

$$
3. g_{33} = \vec{g}_3 \cdot \vec{g}_3 = 1
$$

Definition 4. (Contravariant metric tensor z^{ij}). *The contravariant metric tensor z^{ij} is the matrix inverse of the covariant metric tensor z_{ij}:*

$$
z_{ij} \cdot z^{jk} = z_{ij} \cdot z^{kj} = \delta_k^i,
\tag{11}
$$

where δ_k^i is the Kronecker symbol.

Definition 5. (Contravariant basis z^i). *The contravariant basis $\mathbf{z}^i$ is defined as*

$$
\mathbf{z}^i = z^{ij} \mathbf{z}_j = z^{ji} \mathbf{z}_j
\tag{12}
$$

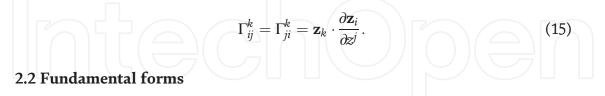The bases $\mathbf{z}_i$ and $\mathbf{z}^i$ are mutually orthonormal:

$$
\mathbf{z}_i \cdot \mathbf{z}^j = \delta_j^i.
\tag{13}
$$

Definition 6. (Christoffel symbol). *In affine and curvilinear coordinate systems, the covariant basis $\mathbf{z}_i$ is the same at all points and varies from one point to another,*

respectively. This variation can be described by the partial derivatives $\partial z_i / \partial z^j$. Using decomposition of partial derivatives $\partial z_i / \partial z^j$ with respect to the covariant basis z_k, the Christoffel symbol Γ_{ij}^{k} is given by

$$\frac{\partial \mathbf{z}_i}{\partial z^j} = \Gamma_{ij}^{k} \mathbf{z}_k. \tag{14}$$

Note that the Christoffel symbol is symmetric in lower indices:

$$\Gamma_{ij}^{k} = \Gamma_{ji}^{k} = \mathbf{z}_k \cdot \frac{\partial \mathbf{z}_i}{\partial z^j}. \tag{15}$$

2.2 Fundamental forms

The *first fundamental form* of the surface is also known as the restriction of the metric tensor to the tangent plane. It is given by its components

$$\mathbf{z}_{ij} = \vec{\mathbf{z}_i} \cdot \vec{\mathbf{z}_j}.$$

Alternatively, its contravariant form is given by

$$\mathbf{z}^{ij} = \vec{\mathbf{z}}^{i} \cdot \vec{\mathbf{z}}^{j}.$$

Note that the first fundamental form can be used for the conversion of covariant components into contravariant components, such as

$$\mathbf{v}^i = \mathbf{z}^{ik} \mathbf{v}_k$$

The Euclidean norm of the two-dimensional tensors is denoted by $\|\cdot\|_{\varepsilon}$ and the corresponding inner product by $< \cdot, \cdot >_{\varepsilon}$. Note that the first fundamental form can be used for the evaluation of such norm quantities:

$$< \underline{u}, \underline{v} >_{\varepsilon} = u_i \mathbf{z}^{ij} v_j, \tag{16}$$

$$\|\underline{v}\|_{\varepsilon}^2 = v_i \mathbf{z}^{ij} v_j, \tag{17}$$

$$< \underline{\underline{T}}, \underline{\underline{U}} > = T_{ij} \mathbf{z}^{ik} \mathbf{z}^{jl} U_{kl}, \tag{18}$$

$$\left\| \underline{\underline{T}} \right\|_{\varepsilon}^2 = T_{ij} \mathbf{z}^{ik} \mathbf{z}^{jl} T_{kl}. \tag{19}$$

The second fundamental form

$$b_{ij} = \mathbf{z}_{\vec{3}} \cdot \mathbf{z}_{\overrightarrow{i,j}},$$

where

$$\mathbf{z}_{\overrightarrow{i,j}} = \frac{\partial^2 \varphi}{\partial \xi^i \partial \xi^j} = \mathbf{z}_{\overrightarrow{j,i}}$$

is the fundamental form of symmetry.

The second fundamental form is yet another important second-order tensor of the surface. It is also known as the *curvature tensor* since it provides information about the curvature of the surface. The values of these curvatures along the

directions are called the *principal curvatures*. The product and the half-sum of the principal curvatures are classically known as the *Gaussian* curvature and *mean* curvature, respectively.

The third fundamental form

$$c_{ij} = b_i^k \, b_{kj}$$

It is a derivative along a curve lying on the surface. Note that the expressions of surface Christoffel symbols and surface covariant derivative are inferred from the third fundamental form.

Remark 1. $z_{\vec{3}} \cdot z_{\vec{3}} = 1 \Rightarrow z_{\overrightarrow{3,i}} \cdot z_{\vec{3}} = 0$ *that is* $z_{\overrightarrow{3,i}}$ *which lies in the tangent plane. Hence, we have*

$$z_{\overrightarrow{3,i}} = \left(z_{\overrightarrow{3,i}} \cdot z_k \right) \overrightarrow{z^k}, \tag{20}$$

and thus

$$z_{\overrightarrow{3,i}} = -b_{ik} \overrightarrow{z^k} = -b_i^k z_{\vec{k}}. \tag{21}$$

The initial tunica intimal lesion in AD is heterogenous in terms of various attributes such as shape, size, and conjugality among others. These notions of surface differential geometry are helpful to model these lesions as higher-order initial lesions. To illustrate, the surface of lesion modeled as initial lesion can be *elliptic*, *parabolic*, or *hyperbolic* according to whether its Gaussian curvature is positive, zero, or negative, respectively. Note that Gaussian curvature is derived from the second fundamental form. From now onwards, we simply use initial lesion model to describe initial lesion of aortic dissection.

3. Modeling of initial lesion

Normally, the aorta is composed of three layers, tunica adventitia, tunica media, and tunica intima (from outside to inside in cross section). Tunica adventitia is composed of linear palisades of collagen fibers as an envelope over tunica media that is a smooth muscle layer, capable of elastic recoil for propelling blood forward. Tunica intima is quite a thin innermost layer comprised of linear array of collagen fibers.

3.1 A simplistic view of initial lesions

To simplify, it is assumed that collagen fibers are straight and resist deformation caused by hemodynamic stresses. In addition, hemodynamic stress, normal to mid-surface of tunica media, is zero throughout the cardiac cycle. The modeling of initial lesion of AD based on the aforementioned kinematical assumptions can be interpreted as a truncation of the expansion of displacements across the thickness of the normal human aorta. The kinematical assumptions pertain to the displacements of points located on tunica intima layer of the aorta through the lesion thickness. Such points are orthogonal to mid-surface in the earlier pre-deformed configuration. Note that the kinematical assumptions connect the displacements of points located on the tunica intima layer that is orthogonal to the mid-surface of the tunica media layer in undeformed configuration. The displacement is expressed by the following equation:

$$\vec{\mathfrak{D}}\left(\xi^1, \xi^2, \xi^3\right) = \vec{d}\left(\xi^1, \xi^2\right) + \xi^3 \vec{\theta}_k\left(\xi^1, \xi^2\right) \vec{z}^k\left(\xi^1, \xi^2\right), \tag{22}$$

In Eq. (22), we consider the tunica intima layer in the direction of $\vec{z}_3$ at the coordinate $\left(\xi^1, \xi^2\right)$. The displacement $\vec{d}\left(\xi^1, \xi^2\right)$ represents a global infinitesimal displacement of the linearly arranged endothelial cells of the tunica intima on the line displacing by the similar amount. The displacement $\xi^3 \vec{\theta}_k\left(\xi^1, \xi^2\right) \vec{z}^k\left(\xi^1, \xi^2\right)$ is due to the rotation of the line measured by θ_1 and θ_2.

Hemodynamic flows can cause both linear and rotational strain. The linear strain is caused by laminar flow, while the rotational strain is caused by either turbulent flow and/or concomitant nonlinear geometry of the vessel. Thus, the measure of linear strain is not sufficient, rather inaccuracies emanate from the increments in rotation. We choose the principle of deformation gradient to calculate both the strains. The combined linear and nonlinear strains can be characterized by stretch tensor called Green-Lagrange strain tensor. The 3D-Lagrange-Green tensor, for which the components $e_{\alpha\beta}$ for general displacement $\vec{\mathfrak{D}}\left(\xi^1, \xi^2, \xi^3\right)$ are

$$e_{\alpha\beta} = \frac{1}{2}\left(\vec{g}_\alpha \cdot \vec{\mathfrak{D}}_{,\beta} + \vec{g}_\beta \cdot \vec{\mathfrak{D}}_{,\alpha}\right), \quad \alpha, \beta = 1, 2, 3. \tag{23}$$

To calculate the components of Green-Lagrange strain tensor, we need to evaluate $\mathfrak{D}_{,\alpha} = \partial\mathfrak{D}/\partial\xi^\alpha$ (displacement of endothelial cells in a line on the tunica intima in ξ^α direction). For the specific displacement in (22), we compute the covariant components of the linearized strain tensor. We have

$$\frac{\partial d}{\partial \xi^i} = \frac{\partial}{\partial \xi^i}\left(d_k \mathbf{z}^k + d_3 \mathbf{z}_3\right) \tag{24}$$

We peruse the fundamental forms to obtain

$$\frac{\partial}{\partial \xi^i}\left(d_k \mathbf{z}^k\right) = \mathbf{z}^k \frac{\partial d_k}{\partial \xi^i} + d_k \frac{\partial \mathbf{z}^k}{\partial \xi^i} = \mathbf{z}^k \frac{\partial d_k}{\partial \xi^i} + b_i^k d_k a_3. \tag{25}$$

Hence,

$$\begin{aligned}
\frac{\partial d}{\partial \xi^i} &= d_{k|i} \mathbf{z}^k + b_i^k d_k \mathbf{z}_3 + d_{3,i} \mathbf{z}_3 + d_3 \mathbf{z}_{3,i} \\
&= \left(d_{k|i} - b_{ki} d_3\right) \mathbf{z}^k + \left(d_{3,i} + b_i^k d_k\right) \mathbf{z}_3,
\end{aligned} \tag{26}$$

where $d_{k|i} = \partial d_k/\partial \xi^i$. As we have calculated the derivative for linearized strain, we calculate the derivative for rotational strain. From (21)

$$\frac{\partial}{\partial \xi^i}\left(\theta_k \mathbf{z}_k\right) = \theta_{k|i} \mathbf{z}_k + b_i^k \theta_k \mathbf{z}_3. \tag{27}$$

The overall displacement in Eq. (22) is composed of linear displacement and rotational displacement. Therefore,

$$\frac{\partial \mathfrak{D}}{\partial \xi^i} = \frac{\partial d}{\partial \xi^i} + \frac{\partial}{\partial \xi^i}\left(\xi^3 \theta_k \mathbf{z}_k\right) = \left(d_{k|i} - b_{ki} \mathbf{z}_3 + \xi^3 \theta_{k|i}\right)\mathbf{z}_k + \left(d_{3,i} + b_i^k d_k + \xi^3 b_i^k \theta_k\right)\mathbf{z}_3. \tag{28}$$

Moreover,

$$\frac{\partial \mathfrak{D}}{\partial \xi^3} = \theta_k \mathbf{z}^k \tag{29}$$

Substituting Eqs. (28), (29), and (7) into (23)

$$\begin{cases} e_{ij} = \gamma_{ij}\left(\vec{d}\right) + \xi^3 \chi_{ij}\left(\vec{d}, \underline{\theta}\right) - \left(\xi^3\right)^2 \kappa_{ij}(\underline{\theta}), & i,j = 1,2 \\ e_{i3} = \zeta_i\left(\vec{d}, \underline{\theta}\right), & i = 1,2 \\ e_{33} = 0, \end{cases} \tag{30}$$

where

$$\begin{cases} \gamma_{ij}\left(\vec{d}\right) & = \frac{1}{2}\left(d_{i|j} + d_{j|i}\right) - b_{ij}\mathbf{z}_3 \\ \chi_{ij}\left(\vec{d}, \underline{\theta}\right) & = \frac{1}{2}\left(\theta_{i|j} + \theta_{j|i} - b_j^k d_{k|i} - b_i^k d_{k|j}\right) + c_{ij}\mathbf{z}_3 \\ \kappa_{ij}(\underline{\theta}) & = \frac{1}{2}\left(b_j^k \theta_{k|i} + b_i^k \theta_{k|j}\right) \\ \zeta_i\left(\vec{d}, \underline{\theta}\right) & = \frac{1}{2}\left(\theta_i + d_{3,i} + b_i^k d_k\right) \end{cases} \tag{31}$$

In the framework of the kinematical assumptions, the second-order tensors, $\underline{\gamma}$ and $\underline{\chi}$, and the first-order tensor $\underline{\zeta}$ are called the membrane strain, bending strain, and shear strain, respectively.

3.2 Higher-order model for initial lesion

In pathological conditions and even in physiological conditions strained to its limits, fluid-structure interaction in the aorta does not follow the kinematical assumptions because the arrangement of collagen fibers in the aortic wall is not straight. Tunica intima is comprised of a single layer of endothelial cells with a subendothelial layer of varying thickness. Tunica intimal surface is nonconformal depending upon the amount of subendothelial ground matrix, contrary to the conventional perspective of the conformal tunica intimal surface. The tunica media is a complex three-dimensional network of smooth muscle cells, elastin, and bundles of collagen fibrils. These well-defined concentrically oriented fibers are mutually reinforcing in radial direction. Tunica adventitia is comprised of fibroblasts, fibrocytes, collagen fibers (helically arranged), and ground matrix.

The constituents of the aortic wall including collagen fibers, elastin fibers, smooth muscle fibers, and ground matrix can stretch to deformation and recoil. Histologically and functionally, these constituents are viscoelastic; hence, aortic tissues resist deformation, albeit partially. Note that hemodynamic strain normal to mid-surface of tunica intima will not be zero.

The assumptions in the simplistic case (22) does not hold true in clinical settings. Thus, an initial lesion model is required to incorporate these attributes. An initial lesion model that is asymptotically consistent with three-dimensional solid mechanics without resorting to any independent kinematical assumptions on the strains requires correction for rotation inaccuracies, while only linearized strain tensor is perused for displacement equation (22). For initial lesion model, the

displacement vector $\overrightarrow{\mathfrak{D}}\left(\xi^1, \xi^2, \xi^3\right)$ contains at least all terms up to degree two, namely,

$$\overrightarrow{\mathfrak{D}}\left(\xi^1, \xi^2, \xi^3\right) = \overrightarrow{d}\left(\xi^1, \xi^2\right) + \xi^3 \overrightarrow{\theta}\left(\xi^1, \xi^2\right) + \left(\xi^3\right)^2 \overrightarrow{\varrho}\left(\xi^1, \xi^2\right). \tag{32}$$

In the simplistic view, the strain normal to the tunica intima is zero since the vessel wall does not deform. In higher-order model, the vector $\overrightarrow{\theta}$ is arbitrary in the Euclidean space and not constrained to lie in the tangential plane. The modified expression for strain components is as follows:

$$\begin{cases} e_{ij}\left(\overrightarrow{\mathfrak{D}}\right) = \gamma_{ij}\left(\overrightarrow{d}\right) + \xi^3 \chi_{ij}\left(\overrightarrow{d}, \overrightarrow{\theta}\right) + \left(\xi^3\right)^2 \kappa_{ij}\left(\overrightarrow{\theta}, \overrightarrow{\varrho}\right) + \left(\xi^3\right)^3 l_{ij}\left(\overrightarrow{\varrho}\right) \\ e_{i3}\left(\overrightarrow{\mathfrak{D}}\right) = \zeta_i\left(\overrightarrow{d}, \overrightarrow{\theta}\right) + \xi^3 m_i\left(\overrightarrow{\theta}, \overrightarrow{\varrho}\right) + \left(\xi^3\right)^2 n_i\left(\overrightarrow{\varrho}\right) \\ e_{33}\left(\overrightarrow{\mathfrak{D}}\right) = \varpi\left(\overrightarrow{\theta}\right) + \xi^3 p\left(\overrightarrow{\varrho}\right) \end{cases} \tag{33}$$

where

$$\begin{cases} \gamma_{ij}\left(\overrightarrow{d}\right) & = \dfrac{1}{2}\left(d_{i|j} + d_{j|i}\right) - b_{ij}d_3 \\ \chi_{ij}\left(\overrightarrow{d}, \overrightarrow{\theta}\right) & = \dfrac{1}{2}\left(\theta_{i|j} + \theta_{j|i} - b_j^k d_{k|i} - b_i^k d_{k|j}\right) - b_{ij}\theta_3 + c_{ij}d_3 \\ \kappa_{ij}\left(\overrightarrow{\theta}, \overrightarrow{\varrho}\right) & = \dfrac{1}{2}\left(\varrho_{i|j} + \varrho_{j|i} - b_j^k \theta_{k|i} - b_i^k \theta_{k|j}\right) - b_{ij}\varrho_3 + c_{ij}\theta_3 \\ l_{ij}\left(\overrightarrow{\varrho}\right) & = -\dfrac{1}{2}\left(b_j^k \varrho_{k|i} + b_i^k \varrho_{k|j}\right) + c_{ij}\varrho_3 \\ \zeta_i\left(\overrightarrow{d}, \overrightarrow{\theta}\right) & = \dfrac{1}{2}\left(\theta_i + d_{3,i} + b_i^k d_k\right) \\ m_i\left(\overrightarrow{\theta}, \overrightarrow{\varrho}\right) & = \dfrac{1}{2}\left(2\varrho_i + \theta_{3,i}\right) \\ n_i\left(\overrightarrow{\varrho}\right) & = \dfrac{1}{2}\left(-b_i^k \varrho_k + \varrho_{3,i}\right) \\ \varpi\left(\overrightarrow{\theta}\right) & = \theta_3 \\ P\left(\overrightarrow{\varrho}\right) & = 2\varrho_3 \end{cases} \tag{34}$$

Here, the tensors, $\underline{\underline{\gamma}}$ and $\underline{\zeta}$, are called the membrane and shear strain tensors as defined in Eq. (31). The tensor $\underline{\underline{\chi}}$ is a generalization of the bending strain tensor, and $\underline{k}$ is a generalization of $-\underline{\underline{\kappa}}$ in Eq. (31), since θ_3 appears in the expressions of $\underline{\chi}$ and $\underline{k}$ in Eq. (34). Because of different orders in ξ^3 in higher-order displacement vector, the newer tensors including $\underline{l}$, $\underline{m}$, $\underline{n}$, $\underline{\varpi}$, and $\underline{p}$ are obtained. In initial lesion model, the different orders in ξ^3 introduces complex interplay of various tensors. The continuous interplay among tensors of different orders makes it difficult to calculate resultant displacement, comprised of linear and rotational displacements. It becomes necessary to peruse algebra for weak formulation of this complex interplay of tensors. The variational formulation using a test function on displacement which aids to evaluate displacement equation in higher-order is

$$\int_\Omega H^{\alpha\beta\lambda\mu} e_{\alpha\beta}\left(\overrightarrow{\mathfrak{D}}\right) e_{\lambda\mu}\left(\overrightarrow{\Delta}\right) dV = \int_\Omega \overrightarrow{F}.\overrightarrow{\Delta} dV, \tag{35}$$

where the function, $\vec{\Delta}\left(\xi^1, \xi^2, \xi^3\right)$, is called test function; for each $\vec{\Delta} \in \mathcal{V}$ (domain for initial lesion) there exists unique $\vec{\mathfrak{D}} \in \mathcal{V}$ such that Eq. (35) holds:

$$\vec{\Delta}\left(\xi^1, \xi^2, \xi^3\right) = \vec{\delta}\left(\xi^1, \xi^2\right) + \xi^3 \vec{\eta}\left(\xi^1, \xi^2\right) + \left(\xi^3\right)^2 \vec{\varsigma}\left(\xi^1, \xi^2\right) \qquad (36)$$

It obviously comes to mind: what are kinematical assumptions in initial lesion model? Keeping the histological and functional perspective of the vessel wall from the biomechanical point of view, it is known that internal surface of the vessel wall is not smooth. It becomes obvious that it will not follow banal kinematical assumptions as mentioned earlier. Note that the initial lesion of AD might be evolving on the tunica intima due to medial degeneration. The lesion presence is spatially nonlinear. It seems plausible that it is governed by quadratic equation as higher-order tensor has quadratic components. The equation for kinematical assumption in higher-order displacement equation, setting $\tau = 2\xi^3/t$, is given by

$$\vec{\mathfrak{D}} = \frac{\tau(\tau - 1)}{2}\vec{d}^{bot} + \left(1 - (\tau)^2\right)\vec{d}^{mid} + \frac{\tau(\tau + 1)}{2}\vec{d}^{top} \qquad (37)$$

Since the internal lining is not smooth, a gestalt view of affected tunica intima has initial lesions at differing heights. Lesions are on the tunica intima surface. To localize spatial dimension of lesions across tunica intima surface, correction terms are to be introduced to tunica intima surface levels, viz. top, mid, and bottom in form of $\tau(\tau - 1)/2$, $1 - (\tau)^2$, and $\tau(\tau + 1)/2$, respectively.

4. Mathematical analysis of initial lesion

We did weak formulation to estimate strain tensors. Now, we assess net displacement. In order to do so, well-posedness of variational form (35) is the key. To understand the evolution of AD, the initial lesion from its inception to the advanced stage wherein the lesion contributes to nonlinear radial dilatation and marginal elongation of diseased aortic tissue needs to be evaluated. There are bounds to emergence of lesion, the lower bound is the status of primal lesion first noticed, and the upper bound is advanced stage of lesion that contributes to rupture of the aorta. Within these bounds, the blood flow acts on the lining of the aorta, adversely impacting the primal lesion that is susceptible to progression from lower bound to upper bound and contributing to the severity of disease.

The inherent nature of normal aortic tissue is to retain its earlier state despite varying interplay of tensors in higher-order. But this resistive tendency, called *coercivity*, weakens as primal lesion progresses towards upper bound. This transition from lower bound to upper bound depends on the complex interplay of various tensors in higher-order. Interestingly, the interplay between tensors in higher-order and coercivity is responsible for worsening of the disease. Intuitively, coercivity is inversely proportional to the progression towards upper bound. Thus, gaining information about the progression towards upper bound and concomitant decline in coercivity is vital to understand net displacement of initial lesion and progression of disease.

For a particular bound and coercivity for a test function $\vec{\Delta}\left(\vec{\delta}, \vec{\eta}, \vec{\varsigma}\right)$, there exists a unique $\vec{\mathfrak{D}}\left(\vec{d}, \vec{\theta}, \vec{\varrho}\right)$, exemplifying a particular state of disease. Furthermore, there are various states of displacement of initial lesion due to progression of the disease.

Such a compendium is used to characterize a particular displacement state. A higher-dimensional space, *Sobolev space* which is comprised of all such possible combinations, comes handy. It is constituted of functions with sufficiently many derivative including partial differential equations of fluid-structure interaction and equipped with the norm that measures size and regularity of these functions. The test function $\vec{\Delta}\left(\vec{\delta},\vec{\eta},\vec{\varsigma}\right)$ is a replica of $\vec{\mathfrak{D}}\left(\vec{d},\vec{\theta},\vec{\varrho}\right)$ in higher-dimensional metric space, $\mathcal{V}$. Since test function is an idealized version of net displacement vector in continuum mechanics, evaluating the interaction between test function $\vec{\Delta}\left(\vec{\delta},\vec{\eta},\vec{\varsigma}\right)$ and force $\vec{F}$ yields insights about $\vec{\mathfrak{D}}\left(\vec{d},\vec{\theta},\vec{\varrho}\right)$. $\vec{\Delta}\left(\vec{\delta},\vec{\eta},\vec{\varsigma}\right)$ is a test function present in Sobolev space. Gaining information about the characteristics of $\vec{\Delta}\left(\vec{\delta},\vec{\eta},\vec{\varsigma}\right)$, we can infer about $\vec{\mathfrak{D}}\left(\vec{d},\vec{\theta},\vec{\varrho}\right)$. It yields insight about the disease process wherein with progression the initial lesion is contributed by the blood flow. Interestingly, proving well-posedness of Eq. (35) gives insights about $\vec{\mathfrak{D}}\left(\vec{d},\vec{\theta},\vec{\varrho}\right)$ present in bilinear function $A\left(\vec{d},\vec{\theta},\vec{\varrho};\vec{\delta},\vec{\eta},\vec{\varsigma}\right)$, which is given by

$$A\left(\vec{d},\vec{\theta},\vec{\varrho};\vec{\delta},\vec{\eta},\vec{\varsigma}\right) = \int_{\Omega} H^{\alpha\beta\lambda\mu}e_{\alpha\beta}\left(\vec{d}+\xi^3\vec{\theta}+\left(\xi^3\right)^2\vec{\varrho}\right)e_{\lambda\mu}\left(\vec{\delta}+\xi^3\vec{\eta}+\left(\xi^3\right)^2\vec{\varsigma}\right)dV. \quad (38)$$

The linear function is given by

$$F\left(\vec{\delta},\vec{\eta},\vec{\varsigma}\right) = \int_{\Omega}\vec{F}.\left(\vec{\delta}+\xi^3\vec{\eta}+\left(\xi^3\right)^2\vec{\varsigma}\right)dV \quad (39)$$

The specification of the displacement space is given by

$$\mathcal{V} = \left\{\left(\vec{\delta},\vec{\eta},\vec{\varsigma}\right)\in H^1(\mathcal{S})\times H^1(\mathcal{S})\times H^1(\mathcal{S})\right\}\cap\mathscr{BC}, \quad (40)$$

where H^1 is the Sobolev space of order 1, $\mathscr{BC}$ is space for boundary conditions.

Lemma 1. *Let us consider* $\vec{\delta}$, $\underline{\eta}\in H^1(\mathcal{S})$ *and*

$$\left(\underline{\underline{\gamma}}\left(\vec{\delta}\right),\underline{\underline{\chi}}\left(\vec{\delta},\underline{\eta}\right),\underline{\zeta}\left(\vec{\delta},\underline{\eta}\right)\right) = \left(\underline{0},\underline{0},\underline{0}\right) \quad on \quad \mathcal{S}. \quad (41)$$

Then, the displacement (36) in $\mathscr{B}$ (higher-dimensional initial lesion body) corresponds to an infinitesimal rigid-body motion, i.e., there exists $\vec{T}$ and $\vec{R}$ a global translation vector and an infinitesimal rotation vector, respectively, such that

$$\vec{\delta}\left(\xi^1,\xi^2\right) = \vec{T}+\vec{R}\wedge\vec{\varphi}\left(\xi^1,\xi^2\right); \qquad \underline{\eta}\left(\xi^1,\xi^2\right) = \vec{R}\wedge z_3\left(\xi^1,\xi^2\right) \quad (42)$$

Lemma 2. *For any* $\left(\xi^1,\xi^2,\xi^3\right)\in\Omega$, *there exist two constants* $\mathfrak{c},C>0$ *such that the following inequalities hold*

$$\mathfrak{c}\sqrt{z\left(\xi^1,\xi^2\right)} \leq \sqrt{g\left(\xi^1,\xi^2,\xi^3\right)} \leq C\sqrt{z\left(\xi^1,\xi^2\right)} \quad (43)$$

$$\mathfrak{c}z^{ij}\left(\xi^1,\xi^2\right)Y_iY_j \leq g^{ij}\left(\xi^1,\xi^2,\xi^3\right)Y_iY_j \leq Cz^{ij}\left(\xi^1,\xi^2\right)Y_iY_j, \quad \forall(Y_1,Y_2)\in\mathbb{R}^2. \quad (44)$$

$$
\begin{aligned}
& \mathfrak{c} \boldsymbol{z}^{ik}\left(\xi^1, \xi^2\right) \boldsymbol{z}^{jl}\left(\xi^1, \xi^2\right) Y_{ij} Y_{kl} \leq g^{ik}\left(\xi^1, \xi^2, \xi^3\right) g^{jl}\left(\xi^1, \xi^2, \xi^3\right) Y_{ij} Y_{kl} \\
& \leq \mathcal{C} \boldsymbol{z}^{ik}\left(\xi^1, \xi^2\right) \boldsymbol{z}^{jl}\left(\xi^1, \xi^2\right) Y_{ij} Y_{kl}, \quad \forall\left(Y_{11}, Y_{12}, Y_{21}, Y_{22}\right) \in \mathbb{R}^4 .
\end{aligned}
\tag{45}
$$

Lemma 3. *The gradient of a vector field is on average not distant from the space of skew-symmetric matrices, the gradient must not be a far from a particular skew-symmetric matrices. Thus, there exists a constant $\delta_k > 0$ such that for any first order surface tensor $\underline{r} \in H^1(\mathcal{S})$,*

$$
|\underline{r}|_{H^1(\mathcal{S})} \leq \delta_k \left(\left\| \underline{\underline{\epsilon}}(r) \right\|_{L^2(\mathcal{S})} + \|\underline{r}\|_{L^2(\mathcal{S})} \right), \quad \text{for } \underline{\underline{\epsilon}}(r) = \frac{1}{2}\left(\underline{\underline{\nabla}} \ \underline{r} + \left(\underline{\underline{\nabla}} \ \underline{r} \right)^T \right),
\tag{46}
$$

where $\underline{\underline{\epsilon}}$ is symmetrized gradient tensor.

It is inferred from Lemma 2 that mapping of initial lesion is well-defined in curvilinear coordinate system wherein quantity g is volume measure. Also, Lemma 2 suggests that this function is well-defined and continuous. Because the initial lesion is defined over upper bound ($\mathcal{C}$) and lower bound ($\mathfrak{c}$), the set of bounds is a compact set. The mid-surface of initial lesion definitely lies within the bounds. Thus, the characterization of initial lesion is well-defined. In order to comment on net displacement of the initial lesion during the progression of disease, we prove the following theorem to establish well-posedness of weak formulation for displacement vector.

Theorem 1. *Assume $\vec{F} \in L^2(\mathcal{B})$; the essential boundary conditions enforced in $\mathcal{V}$ are such that no rigid-body motion is possible, i.e., the only element $\left(\vec{\delta}, \vec{\eta}, \vec{\varsigma}\right)$ in $\mathcal{V}$ satisfies Eq. (42) for some $\left(\vec{T}, \vec{R}\right)$ is $\left(\vec{0}, \vec{0}, \vec{0}\right)$.*

Then there exists a unique $\left(\vec{d}, \vec{\theta}, \vec{\varrho}\right)$ in $\mathcal{V}$ that satisfies

$$
A\left(\vec{d}, \vec{\theta}, \vec{\varrho}; \vec{\delta}, \vec{\eta}, \vec{\varsigma}\right) = F\left(\vec{\delta}, \vec{\eta}, \vec{\varsigma}\right)
\tag{47}
$$

for any $\left(\vec{\delta}, \vec{\eta}, \vec{\varsigma}\right) \in \mathcal{V}$, and we have

$$
\left\| \vec{d}, \vec{\theta}, \vec{\varrho} \right\|_1 \leq \mathcal{C} \left\| \vec{F} \right\|_{L^2(\mathcal{B})}
\tag{48}
$$

Proof. We prove coercivity of A and continuity of A and F. Coercivity argument is explained in three steps. We shall write f instead of function $f(,)$ to make equations more compact.

(i) First, we prove

$$
A\left(\vec{d}, \vec{\eta}, \vec{\varsigma}; \vec{\delta}, \vec{\eta}, \vec{\varsigma}\right) \geq \gamma \left(\left\| \underline{\underline{\gamma}} \right\|_0^2 + \left\| \underline{\underline{\chi}} \right\|_0^2 + \left\| \underline{\underline{k}} \right\|_0^2 + \left\| \underline{\underline{l}} \right\|_0^2 + \left\| \underline{\varsigma} \right\|_0^2 + \left\| \underline{m} \right\|_0^2 + \left\| \underline{n} \right\|_0^2 + \left\| \varpi \right\|_0^2 + \left\| p \right\|_0^2 \right).
\tag{49}
$$

From Eqs. (44) and (45), using $g^{\alpha\beta} g^{\lambda\mu} e_{\alpha\beta} e_{\lambda\mu} = \left(g^{\alpha\beta} e_{\alpha\beta}\right)^2 \geq 0$, we have

$$
\begin{aligned}
A\left(\vec{d}, \vec{\eta}, \vec{\varsigma}; \vec{\delta}, \vec{\eta}, \vec{\varsigma}\right) & \geq \gamma \int_\Omega g^{\alpha\beta} g^{\lambda\mu} e_{\alpha\beta} e_{\lambda\mu} dV \\
& \geq \gamma \int_\Omega \left[g^{ik} g^{jl} e_{ij} e_{kl} + g^{ij} e_{i3} e_{j3} + \left(e_{33}\right)^2 \right] dV \\
& \geq \gamma \int_\Omega \left[\mathbf{z}^{ik} \mathbf{z}^{jl} e_{ij} e_{kl} + \mathbf{z}^{ij} e_{i3} e_{j3} + \left(e_{33}\right)^2 \right] dV
\end{aligned}
\tag{50}
$$

Now using Eqs. (43) and (33) and integrating through the thickness, we obtain

$$
A\left(\vec{d}, \vec{\eta}, \vec{\varsigma}; \vec{\delta}, \vec{\eta}, \vec{\varsigma}\right) \geq \gamma \int_{\omega} t \{ \mathbf{z}^{ik}\mathbf{z}^{jl} [\gamma_{ij}\gamma_{kl} + \frac{t^2}{12}\chi_{ij}\chi_{kl} + \frac{t^2}{6}\gamma_{ij}k_{kl}
$$
$$
+ \frac{t^4}{80}k_{ij}k_{kl} + \frac{t^4}{40}l_{ij}\chi_{kl} + \frac{t^6}{448}l_{ij}l_{kl}] + \left[\varpi^2 + \frac{t^2}{12}p^2\right] \tag{51}
$$
$$
+ \mathbf{z}^{ij}\left[\zeta_i\zeta_j + \frac{t^2}{12}m_im_j + \frac{t^2}{6}\zeta_in_j + \frac{t^4}{80}n_in_j\right]\}dS
$$

To simplify the above expression, we use the following inequality:

$$
|ab| \leq \frac{1}{2}\left(\eta a^2 + \frac{1}{\eta}b^2\right), \quad \forall \eta > 0. \tag{52}
$$

Now we have

$$
|\frac{t^2}{6}\mathbf{z}^{ik}\mathbf{z}^{jl}\gamma_{ij}k_{kl}| = \frac{1}{6}|\langle\gamma, t^2 k\rangle|
$$
$$
\leq \frac{1}{12}\left(a_1\|\gamma\|_{\varepsilon}^2 + \frac{t^4}{a_1}\|k\|_{\varepsilon}^2\right) \tag{53}
$$
$$
\leq \frac{1}{12}\mathbf{z}^{ik}\mathbf{z}^{jl}\left(a_1\gamma_{ij}k_{kl} + \frac{t^4}{a_1}k_{ij}k_{kl}\right),
$$

and similarly

$$
|\frac{t^4}{40}\mathbf{z}^{ik}\mathbf{z}^{jl}l_{ij}\chi_{kl}| \leq \frac{1}{80}\mathbf{z}^{ik}\mathbf{z}^{jl}\left(a_2t^6l_{ij}l_{kl} + \frac{t^2}{a_2}\chi_{ij}\chi_{kl}\right). \tag{54}
$$
$$
|\frac{t^2}{6}\mathbf{z}^{ij}\zeta_in_j| \leq \frac{1}{12}\mathbf{z}^{ij}\left(a_3\zeta_i\zeta_j + \frac{t^4}{a_3}n_in_j\right), \tag{55}
$$

where $a_1, a_2, a_3 > 0$. Using suitable values of the constants, $a_1 = a_3 = 10$, $a_2 = 6/35$, and $t > 0$, Eq. (51) becomes

$$
A\left(\vec{d}, \vec{\eta}, \vec{\varsigma}; \vec{\delta}, \vec{\eta}, \vec{\varsigma}\right) \geq \gamma \int_{\omega} \{\mathbf{z}^{ik}\mathbf{z}^{jl}\left[\gamma_{ij}\gamma_{kl} + \chi_{ij}\chi_{kl} + k_{ij}k_{kl} + l_{ij}l_{kl}\right]
$$
$$
+ \mathbf{z}^{ij}\left[\zeta_i\zeta_j + m_im_j + n_in_j\right] + \left[\varpi^2 + p^2\right]\}dS \tag{56}
$$

Hence, Eq. (49) is proved. The bilinear function is bounded below by the sum of norm of strain tensors. This function for mid-surface is integrated through the thickness of the entire lesion giving semblance of the whole lesion.

(ii) Denoting

$$
\|\eta_3, \vec{\varsigma}\|_* = \left(\left\|\underline{m}\left(\vec{\eta}, \vec{\varsigma}\right)\right\|_0^2 + \left\|\underline{n}\left(\vec{\varsigma}\right)\right\|_0^2 + \left\|\underline{k}\left((\underline{0}, \eta_3), \vec{\varsigma}\right)\right\|_0^2 + \left\|\varpi\left(\vec{\eta}\right)\right\|_0^2 + \left\|p\left(\vec{\varsigma}\right)\right\|_0^2\right)^{1/2}
$$
$$
\tag{57}
$$

We now show that $\|\cdot\|_*$ provides a norm equivalent to the H^1-norm over certain subspace of the Sobolev space. Note that $\varpi\left(\vec{\eta}\right) = p\left(\vec{\varsigma}\right) = 0$ gives $\eta_3 = \varsigma_3 = 0$ and $\underline{m}\left(\vec{\eta}, \vec{\varsigma}\right) = \eta_3 = 0$ gives $\underline{\varsigma} = 0$. Bounding the norm from above, we get

$$\left\| \eta_3, \vec{\varsigma} \right\|_* \leq C \left\| \eta_3, \vec{\varsigma} \right\|_1 \tag{58}$$

and we get

$$\left\| \eta_3, \vec{\varsigma} \right\|_* \leq \gamma \left\| \eta_3, \vec{\varsigma} \right\|_1 \tag{59}$$

Using Lemma 3 and Eq. (34), we have

$$
\begin{aligned}
\left| \underline{\varsigma} \right|_1^2 &\leq C \left(\left\| \underline{\varepsilon}(\underline{\varsigma}) \right\|_0^2 + \left\| \underline{\varsigma} \right\|_0^2 \right) \\
&\leq C \left(\left\| \underline{\underline{k}}((\underline{0}, \eta_3), \vec{\varsigma}) \right\|_0^2 + \left\| \underline{\underline{b}}\varsigma_3 \right\|_0^2 + \left\| \underline{\underline{c}}\eta_3 \right\|_0^2 + \left\| \underline{\varsigma} \right\|_0^2 \right) \\
&\leq C \left(\left\| \underline{\underline{k}}\left((\underline{0}, \eta_3), \vec{\varsigma}\right) \right\|_0^2 + \|\varsigma_3\|_0^2 + \|\eta_3\|_0^2 + \|\underline{\varsigma}\|_0^2 \right)
\end{aligned}
\tag{60}
$$

In addition, from the definition of $\underline{n}$ and $\underline{m}$ in Eq. (34), we have

$$\left| \varsigma_3 \right|_1^2 \leq C \left(\left\| \underline{n}\left(\vec{\varsigma}\right) \right\|_0^2 + \left\| \underline{\varsigma} \right\|_0^2 \right) \tag{61}$$

$$\left| \eta_3 \right|_1^2 \leq C \left(\left\| \underline{m}\left(\vec{\eta}, \vec{\varsigma}\right) \right\|_0^2 + \left\| \underline{\varsigma} \right\|_0^2 \right) \tag{62}$$

From Eqs. (60)–(62), we obtain

$$
\begin{aligned}
\left\| \eta_3, \underline{\varsigma} \right\|_1^2 &\leq C \big(\left\| \underline{m}\left(\vec{\eta}, \vec{\varsigma}\right) \right\|_0^2 + \left\| \underline{k}(\underline{0}, \eta), \vec{\varsigma}) \right\|_0^2 \\
&\quad + \left\| \underline{n}\left(\vec{\varsigma}\right) \right\|_0^2 + \|\varsigma_3\|_0^2 + \|\eta_3\|_0^2 + \|\underline{\varsigma}\|_0^2 \big) \\
&\leq C \left(\left\| \eta_3, \vec{\varsigma} \right\|_*^2 + \left\| \eta_3, \vec{\varsigma} \right\|_0^2 \right).
\end{aligned}
\tag{63}
$$

Perusing the norm of the gradient of vector fields, the setting of lower and upper bounds is tantamount to estimating attributes of lesion at the initial and advanced stages, respectively. The sequence of all lower bounds corresponds to the initial stage of disease prevalent in affected population. Similarly, the sequence of all upper bounds corresponds to the advanced stage of disease prevalent in terminally ill patients. Note that each of these sequences is uniformly bounded in the H^1-norm. There exist a subsequence that converges to some limit for each of these sequences. The weak convergence in H^1 implies strong convergence in L^2 for the same norm to the same limit. Thus, the subsequence in L^2-norm converges strongly. This gives a stronger result about the sequences of upper and lower bounds. Clinically, it indicates various patients might report, at different stages of disease owing to different reasons, their disease initiation be an element, which is a limit point of the subsequence of lower bound sequence. Note that primal lesion presence in any patient whatsoever can be traced back by the convergence of subsequence of lower bound sequence. Its corollary equivalently applies to the advanced stage of the disease.

(iii) Coercivity bound: Coercivity is the measure of the ability of the initial lesion to withstand an external fluid-structure interaction without undergoing deformation. It is obviously dependent on the intensity of hemodynamic forces applied to the lesion. Thus, coercivity bound is the limit point of the ability of initial lesion to withstand deformation. Note that in due course of the progression of the disease, the evolution of the lesion at each stage is dependent on the increment of coercivity bound. In normal circumstances, it

seems plausible that with ascension towards upper bound, coercivity reduces. Thus, the evaluation of coercivity bound is relevant.

The inequality (52) is valid for any norm. Hence, we infer

$$\left\| \vec{v}_1 + \alpha \vec{v}_2 \right\|^2 + \left\| \vec{v}_2 \right\|^2 \geq \gamma \left(\left\| \vec{v}_1 \right\|^2 + \left\| \vec{v}_2 \right\|^2 \right), \tag{64}$$

where α is any real number. Using this inequality (64), we obtain

$$\begin{aligned}
\left\| \underline{\underline{\chi}} \left(\vec{\delta}, \vec{\eta} \right) \right\|_0^2 + \left\| \varpi \left(\vec{\eta} \right) \right\|_0^2 &= \left\| \underline{\underline{\chi}} (\vec{\delta}, (\eta, 0) - \underline{b} \eta_3 \right\|_0^2 + \|\eta_3\|_0^2 \\
&\geq \gamma \left(\underline{\underline{\chi}} \left(\vec{\delta}, (\eta, 0) \right) \right) \Big\|_0^2 + \|\eta_3\|_0^2,
\end{aligned} \tag{65}$$

hence,

$$\begin{aligned}
\left\| \underline{\underline{\gamma}} \left(\vec{\delta} \right) \right\|_0^2 + \left\| \underline{\underline{\chi}} \left(\vec{\delta}, \vec{\eta} \right) \right\|_0^2 + \left\| \underline{\underline{\zeta}} \left(\vec{\delta}, \vec{\eta} \right) \right\|_0^2 + \left\| \varpi \left(\vec{\eta} \right) \right\|_0^2 &\geq \gamma (\left\| \underline{\underline{\gamma}} \left(\vec{\delta} \right) \right\|_0^2 + \left\| \underline{\underline{\zeta}} \left(\vec{\delta}, \vec{\eta} \right) \right\|_0^2 \\
+ \left\| \underline{\underline{\chi}} (\vec{\delta}, (\eta, 0)) \right\|_0^2 + \|\eta_3\|_0^2 &\geq \gamma \left(\left\| \vec{\delta}, \eta \right\|_1^2 + \|\eta_3\|_0^2 \right)
\end{aligned} \tag{66}$$

Suppose $\vec{F} \in L^2(\mathcal{S})$ and the essential boundary conditions enforced in $\mathcal{V}$ are such that no rigid-body motion is possible, i.e., the only element $\left(\vec{\delta}, \underline{\eta} \right) \in \mathcal{V}$ satisfying (42) for some $\left(\vec{T}, \vec{R} \right) = \left(\vec{0}, \underline{0} \right)$. Then bilinear form $\mathcal{A}$ is coercive over $\mathcal{V}$.

$$\left\| \underline{\underline{k}} \left(\vec{\eta}, \vec{\varsigma} \right) \right\|_0^2 + |\underline{\eta}|_1^2 \geq \gamma \left(\left\| \underline{\underline{k}} \left((\underline{0}, \eta_3), \vec{\varsigma} \right) \right\|_0^2 + \left| \underline{\eta} \right|_1^2 \right) \tag{67}$$

hence,

$$\begin{aligned}
\left\| \underline{\underline{k}} \left(\vec{\eta}, \vec{\varsigma} \right) \right\|_0^2 &+ \left| \underline{\eta} \right|_1^2 + \|\underline{m}(\vec{\eta}, \vec{\varsigma})\|_0^2 + \left\| \underline{n} \left(\vec{\varsigma} \right) \right\|_0^2 + \left\| \varpi \left(\vec{\eta} \right) \right\|_0^2 + \left\| p \left(\vec{\varsigma} \right) \right\|_0^2 \\
&\geq \gamma \left(\left\| \underline{\underline{k}} ((\underline{0}, \eta_3), \vec{\varsigma}) \right\|_0^2 + \|\underline{m}(\vec{\eta}, \vec{\varsigma})\|_0^2 + \left\| \underline{n} \left(\vec{\varsigma} \right) \right\|_0^2 + \left\| \varpi \left(\vec{\eta} \right) \right\|_0^2 + \left\| p \left(\vec{\varsigma} \right) \right\|_0^2 + \left| \underline{\eta} \right|_1^2 \right) \\
&= \gamma \left(\|\eta_3, \vec{\varsigma}\|_*^2 + \left| \underline{\eta} \right|_1^2 \right) \\
&\geq \gamma \left(\|\eta_3, \vec{\varsigma}\|_1^2 + \left| \underline{\eta} \right|_1^2 \right).
\end{aligned} \tag{68}$$

Therefore, from Eqs. (49), (66), and (68), we have

$$\begin{aligned}
A \left(\vec{d}, \vec{\eta}, \vec{\varsigma}; \vec{\delta}, \vec{\eta}, \vec{\varsigma} \right) &\geq \gamma \left(\|\gamma\|_0^2 + \|\chi\|_0^2 + \|k\|_0^2 + \|l\|_0^2 + \|\zeta\|_0^2 + \|m\|_0^2 + \|n\|_0^2 + \|\varpi\|_0^2 + \|p\|_0^2 \right) \\
&\geq \gamma \left(\left\| \vec{\delta}, \underline{\eta} \right\|_1^2 + \|\eta_3\|_0^2 \left\| \underline{\underline{k}} \right\|_0^2 + \|m\|_0^2 + \|n\|_0^2 + + \|p\|_0^2 \right) \\
&\geq \gamma \left(\left\| \vec{\delta}, \underline{\eta} \right\|_1^2 + \|\eta_3, \vec{\varsigma}\|_1^2 \right) = \gamma \left\| \vec{\delta}, \vec{\eta}, \vec{\varsigma} \right\|_1^2.
\end{aligned} \tag{69}$$

The analysis about coercivity bound suggested that it is not membrane strain tensor alone which progressively alters the structural characteristics of the initial

16

lesion. Rather it is the complex interplay of various tensors in Eq. (34) that breaks the coercivity bound at a particular stage of the disease.

(iv) Completion of the proof.

Since we have proved boundedness and coercivity of the initial lesion, the continuity of the variational formulation can be derived from the continuity of linear function (39) related to test function $\vec{\Delta}\left(\vec{\delta}, \vec{\eta}, \vec{\varsigma}\right)$. There is merit in proving the continuity of variational formulation because such continuous functions within closed interval are bounded:

$$\left| \int_{\Omega} \vec{F} \cdot \left(\vec{\delta} + \xi^3 \vec{\eta} + \left(\xi^3\right)^2 \vec{\varsigma}\right) dV \right| \le \left\| \vec{F} \right\|_{L^2(\mathscr{B})} \left\| \vec{\delta} + \xi^3 \vec{\eta} + \left(\xi^3\right)^2 \vec{\varsigma} \right\|_{L^2(\mathscr{B})}$$

$$\le \left\| \vec{F} \right\|_{L^2(\mathscr{B})} \left\| \vec{\delta}, \vec{\eta}, \vec{\varsigma} \right\|_0 . \tag{70}$$

Then, from the H^1-coercivity of A infer

$$\gamma \left\| \vec{d}, \vec{\theta}, \vec{\varrho} \right\|_1^2 \le A\left(\vec{d}, \vec{\theta}, \vec{\varrho}; \vec{d}, \vec{\theta}, \vec{\varrho}\right) = F\left(\vec{d}, \vec{\theta}, \vec{\varrho}\right) \le C \left\| \vec{F} \right\|_{L^2(\mathscr{B})} \left\| \vec{d}, \vec{\theta}, \vec{\varrho} \right\|_0 . \tag{71}$$

Hence, we infer Eq. (48) directly follows. ◻

The primary result of this section is sufficient conditions for the variational formulation (35) which is proved well-posed. In initial lesion model, a fluid-structure interaction modeled by using bilinear and linear functions specified over displacement is well-posed. Any transverse point-wise loading in H^1 for any lesion implies transverse displacement in H^1. Clinically, progressive interaction of various tensors within lower and upper bounds implies changes in coercivity bounds. It is suggestive of progression of the disease. On the other hand, a fracture in internal lining of vessel wall around the lesion causing blood to flow between tunica intima and tunica media. This flow either remains static (if there is non-patent false lumen) or flow out (if there is a patent false lumen track). Thus, the merit of well-posedness of variational formulation (35) cannot be overemphasized.

5. Asymptotic analysis of the initial lesion

We aim to discuss the asymptotic behavior of initial lesion model. The initial lesion continues to temporally evolve under the influence of fluid-structure inter-action; the asymptotic analysis is helpful in this regard. The nonlinearity of progression of the disease can be assessed by formulating bending strain cases because membrane and shear strain vanish with the strain $\varpi(\eta)$, wherein $\eta \equiv 0$ for the test function $\vec{\Delta}\left(\vec{\delta}, \vec{\eta}, \vec{\varsigma}\right)$ in space $\mathcal{V}$. Let us introduce the space of pure-bending displacements:

$$\mathcal{V}_0 = \left\{ \left(\vec{\delta}, \vec{\eta}, \vec{\varsigma}\right) \in \mathcal{V}, \mid \gamma_{ij}\left(\vec{\delta}\right) = 0, \ \zeta_i\left(\vec{\delta}, \vec{\eta}\right) = 0 \ \ \forall \ i, j = 1, 2 \right\}. \tag{72}$$

Based on peculiar geometry and associated bounds, the initial lesion may or may not have nonzero pure-bending displacements. Situation 1, when pure bending is inhibited

$$\mathcal{V}_0 \cap \left\{ \left(\vec{\delta}, \vec{\eta}, \vec{\varsigma} \right) \in \mathcal{V} \right\} = \{(0, 0, 0)\}, \tag{73}$$

and situation 2, when pure bending is non-inhibited

$$\mathcal{V}_0 \cap \left\{ \left(\vec{\delta}, \vec{\eta}, \vec{\varsigma} \right) \in \mathcal{V} \right\} \neq \{(0, 0, 0)\}, \tag{74}$$

Let us define higher-dimensional body force as

$$\vec{F} = \varepsilon^{(\rho - 1)} \vec{G}, \tag{75}$$

where the exponent $(\rho - 1)$ is used for consistency when the external work involves an integration over the thickness which is relevant for general asymptotic analysis; $\vec{G}$ represents a force field:

$$\vec{G}(\xi^1, \xi^2, \xi^3) = \vec{G}_0(\xi^1, \xi^2) + \xi^3 \vec{B}(\xi^1, \xi^2, \xi^3), \tag{76}$$

where $\vec{G}_0$ is in $L^2(\mathcal{S})$ and $\vec{B}$ is a uniformly bounded function over $\mathscr{B}$ in t. Since it is improbable to obtain strong convergence result in context of asymptotic analysis, we make weaker assumption about $\vec{G}$. We also forgo regularity assumption in context of weak convergence to introduce abstract bilinear forms. Depending upon boundary conditions, nonzero pure-bending displacements of initial lesion are assessed. The displacement is in response to inhibited and non-inhibited pure-bending lesion as we have already argued that only bending strain matters in asymptotic analysis. In the current framework of asymptotic analysis for initial lesion of a given thickness, specific membrane-dominated bilinear form is given by

$$A_m\left(\vec{d}, \vec{\theta}; \vec{\delta}, \vec{\eta}\right) = \int_\omega l[^0H^{ijkl}\gamma_{ij}\left(\vec{d}\right)\gamma_{kl}\left(\vec{\delta}\right) + {}^0H^{ij33}\left(\gamma_{ij}\left(\vec{d}\right)\varpi\left(\vec{\eta}\right) + \gamma_{ij}\left(\vec{\delta}\right)\varpi\left(\vec{\theta}\right)\right)$$
$$+ 4{}^0H^{i3j3}\zeta_i\left(\vec{d}, \vec{\theta}\right)\zeta_j\left(\vec{d}, \vec{\eta}\right) + {}^0H^{3333}\varpi\left(\vec{\theta}\right)\varpi\left(\vec{\eta}\right)]dS, \tag{77}$$

bending-dominated bilinear form is given by

$$A_b\left(\vec{d}, \vec{\theta}, \vec{\varrho}; \vec{\delta}, \vec{\eta}, \vec{\varsigma}\right) = \int_\omega \frac{l^3}{12}{}^0H^{ijkl}\chi_{ij}\left(\vec{d}, \vec{\theta}\right)\chi_{kl}\left(\vec{\delta}, \vec{\eta}\right) + {}^0H^{ij33}\left(\chi_{ij}\left(\vec{d}, \vec{\theta}\right)p\left(\vec{\varsigma}\right) + \chi_{ij}\left(\vec{\delta}, \vec{\eta}\right)p\left(\vec{\varrho}\right)\right)$$
$$+ 4{}^0H^{i3j3}m_i\left(\vec{\theta}, \vec{\varrho}\right)m_j\left(\vec{\eta}, \vec{\varsigma}\right) + {}^0H^{3333}p\left(\vec{\varrho}\right)p\left(\vec{\varsigma}\right)]dS, \tag{78}$$

where the tensor ${}^0H$ is defined by

$$^0H^{\alpha\beta\lambda\mu} = H^{\alpha\beta\lambda\mu}\big|_{\xi^3 = 0},$$

and linear form is given by

$$G\left(\vec{\delta}\right) = \int_\omega l\vec{G}_0 \cdot \vec{\delta} dS.$$

We now discuss the cases of non-inhibited pure bending versus inhibited pure bending.

5.1 The impact of non-inhibited pure bending on the initial lesion

Assume that $\mathcal{V}$ displacement space for the initial lesion contains few nonzero elements. The terms of order zero in ξ^3 in the strain Eq. (33) vanishes by a penalization mechanism, and the appropriate scaling factor is then $\rho = 3$. We define the norm

$$\left\| \vec{\delta}, \vec{\eta}, \vec{\varsigma} \right\|_b = \left(\left\| \vec{\delta} \right\|_1^2 + \left\| \underline{\eta} \right\|_1^2 + \|\eta_3\|_0^2 + \|\varsigma_3\|_0^2 + \left\| \varsigma + \frac{1}{2}\underline{\nabla}\eta_3 \right\|_0^2 \right)^{\frac{1}{2}} \qquad (79)$$

for which the convergence is anticipated. Since $\left(\vec{d^\varepsilon}, \vec{\theta^\varepsilon}, \vec{\rho^\varepsilon} \right)$ is uniformly bounded in the norm $\|\cdot\|_b$, we extract a subsequence weakly converging in $\mathcal{V}$ to a limit $\left(\vec{d^w}, \vec{\theta^w}, \vec{\varrho^w} \right)$. Since in the early stage of the disease, the internal lining of the vessel wall, tunica intima, is smooth, we can expand the constitutive tensor:

$$H^{\alpha\beta\lambda\mu}\left(\xi^1, \xi^2, \xi^3\right) = {}^0H^{\alpha\beta\lambda\mu}\left(\xi^1, \xi^2\right) + \xi^3\overline{H}^{\alpha\beta\lambda\mu}\left(\xi^1, \xi^2, \xi^3\right), \qquad (80)$$

where $\overline{H}^{\alpha\beta\lambda\mu}\left(\xi^1, \xi^2, \xi^3\right)$ is bounded over initial lesion body $\mathcal{B}$. Using the uniform boundedness of $\varepsilon\left\|\vec{d^\varepsilon}, \vec{\theta^\varepsilon}, \vec{\varrho^\varepsilon}\right\|_1$, we get

$$\lim_{\varepsilon\to 0} \frac{1}{\varepsilon}A\left(\vec{d^\varepsilon}, \vec{\theta^\varepsilon}; \vec{\rho^\varepsilon}, \vec{\delta}, \vec{\eta}, \vec{\varsigma}\right) = A_m\left(\vec{d^w}, \vec{\theta^w}; \vec{\delta}, \vec{\eta}\right), \qquad (81)$$

where A_m is the bilinear form to assess net displacement caused by the membrane strain. This is equivalent to

$$\left| \frac{1}{\varepsilon}A\left(\vec{d^\varepsilon}, \vec{\theta^\varepsilon}, \vec{\varrho^\varepsilon}; \vec{\delta}, \vec{\eta}, \vec{\varsigma}\right) \right| = \left| \frac{1}{\varepsilon}\int_\Omega \vec{F}.\left(\vec{\delta} + \xi^3\vec{\eta} + \left(\xi^3\right)^2\vec{\varsigma}\right)dV \right|$$
$$\leq C\varepsilon^2\left\|\vec{\delta}, \vec{\eta}, \vec{\varsigma}\right\|_b + C\varepsilon^2\left\|\vec{\delta}, \vec{\eta}, \vec{\varsigma}\right\|_0. \qquad (82)$$

When $\left(\vec{\delta}, \vec{\eta}, \vec{\varsigma}\right)$ is fixed in $\mathcal{V}$, we get

$$A_m\left(\vec{d^w}, \vec{\theta^w}; \vec{\delta}, \vec{\eta}\right) = 0 \qquad \forall\left(\vec{\delta}, \vec{\eta}, \vec{\varsigma}\right) \in \mathcal{V}. \qquad (83)$$

Using equivalence relations among norms and semi-norms, infer that $\left(\vec{d^w}, \vec{\theta^w}, \vec{\varrho^w}\right) \in \mathcal{V}$. This result (83) shows that bilinear form for the membrane strain tensor vanishes. In this case, non-inhibited pure bending, bending strain tensor predominates whose bilinear form is given by

$$A_b\left(\vec{d^w}, \vec{\theta^w}, \vec{\varrho^w}; \vec{\delta}, \vec{\eta}, \vec{\varsigma}\right) = G\left(\vec{\delta}\right), \qquad \forall\left(\vec{\delta}, \vec{\eta}, \vec{\varsigma}\right) \in \mathcal{V}_0. \qquad (84)$$

Eq. (84) equivalently holds for any $\left(\vec{\delta}, \vec{\eta}, \vec{\varsigma}\right) \in \mathcal{V}_0$ (pure-bending subspace of initial lesion). The uniqueness of solution implies that $\left(\vec{d}^w, \vec{\theta}^w, \vec{\varrho}^w\right) = \left(\vec{d}^0, \vec{\theta}^0, \vec{\varrho}^0\right)$. If Eq. (83) equivalently holds for any weakly converging subsequence $\left(\vec{d}^w, \vec{\theta}^w, \vec{\varrho}^w\right)$, we affirmatively conclude that the whole sequence converges weakly to $\left(\vec{d}^0, \vec{\theta}^0, \vec{\varrho}^0\right)$.

5.2 The impact of inhibited pure bending on the initial lesion

We define pure-bending subspace $\mathcal{V}^{\#}$, of displacement space $\mathcal{V}$ for initial lesion such that

$$\mathcal{V}^{\#} = \left\{ \left(\vec{\delta}, \vec{\eta}\right) \mid \left(\vec{\delta}, \vec{\eta}, \vec{0}\right) \in \mathcal{V} \right\}.$$

In this case, pure bending is inhibited; $\|\cdot\|_m$ gives a norm in pure-bending subspace $\mathcal{V}^{\#}$ such that

$$\left\|\vec{\delta}, \vec{\eta}\right\|_m = \left\|\underline{\underline{\gamma}}\left(\vec{\delta}\right)\right\|_0 + \left\|\underline{\varsigma}\left(\vec{\delta}, \vec{\eta}\right)\right\|_0 + \left\|\varpi\left(\vec{\eta}\right)\right\|_0.$$

Since $\left(\vec{d}^{\varepsilon}, \vec{\theta}^{\varepsilon}\right)$ is uniformly bounded in pure membrane subspace of displacement space for initial lesion, $\varepsilon^2\left(\vec{\delta}, \vec{\eta}, \vec{\varsigma}\right)$ is uniformly bounded in $H^1(\mathcal{S})$; we infer that the sequence $\left(\vec{d}^{\varepsilon} + \frac{t^2}{12}\vec{\varsigma}, \vec{\theta}^{\varepsilon}\right)$ is also uniformly bounded in $\mathcal{V}$. Due to the weak convergence in pure membrane subspace $\mathcal{V}_m$,

$$\left(\underline{\underline{\gamma}}\left(\vec{d}^{\varepsilon} + \frac{t^2}{12}\vec{\varrho}^{\varepsilon}\right), \underline{\varsigma}\left(\vec{d}^{\varepsilon} + \frac{t^2}{12}\vec{\varrho}^{\varepsilon}, \vec{\theta}^{\varepsilon}\right), \varpi\left(\vec{\theta}^{\varepsilon}\right)\right) \overset{\varepsilon \to 0}{\to} \left(\underline{\underline{\gamma}}\left(\vec{d}^w\right), \underline{\varsigma}\left(\vec{d}^w, \vec{\theta}^w\right), \varpi\left(\vec{\theta}^w\right)\right),$$

converges weakly in $L^2(\mathcal{S})$. Hence, for any fixed $\left(\vec{\delta}, \vec{\eta}, \vec{\varsigma}\right)$ in displacement space $\mathcal{V}$, we infer

$$\lim_{\varepsilon \to 0} \frac{1}{\varepsilon} A\left(\vec{d}^{\varepsilon}, \vec{\theta}^{\varepsilon}, \vec{\varrho}^{\varepsilon}; \vec{\delta}, \vec{\eta}, \vec{\varsigma}\right) = A_m\left(\vec{d}^w, \vec{\theta}^w; \vec{\delta}, \vec{\eta}\right). \tag{85}$$

We have

$$\frac{1}{\varepsilon} A\left(\vec{d}^{\varepsilon}, \vec{\theta}^{\varepsilon}, \vec{\varrho}^{\varepsilon}; \vec{\delta}, \vec{\eta}, \vec{\varsigma}\right) = G\left(\vec{\delta}\right) + \frac{R}{\varepsilon}. \tag{86}$$

Here, $\frac{R}{\varepsilon} \to 0$ when $\varepsilon \to 0$. As $\left(\vec{\delta}, \vec{\eta}, \vec{\varsigma}\right)$ is fixed, we infer

$$A_m\left(\vec{d}^w, \vec{\theta}^w; \vec{\delta}, \vec{\eta}\right) = G\left(\vec{\delta}\right) \qquad \forall\left(\vec{\delta}, \vec{\eta}\right) \in \mathcal{V}. \tag{87}$$

Eq. (87) equivalently holds for any $\left(\vec{\delta}, \vec{\eta}\right) \in \mathcal{V}_m$ (membrane subspace of initial lesion). From the uniqueness of the weak convergence result, it follows that $\left(\vec{d}^w, \vec{\theta}^w\right) = \left(\vec{d}^m, \vec{\theta}^m\right)$. If this equivalently holds for any weakly converging

subsequence $\left(\vec{d}^{w}, \vec{\theta}^{w}, \vec{\varrho}^{w}\right)$, we affirmatively conclude that the whole sequence $\left(\vec{d}^{\varepsilon} + \frac{t^2}{12}\vec{\varsigma}, \vec{\theta}^{\varepsilon}\right)$ converges weakly to $\left(\vec{d}^{m}, \vec{\theta}^{m}\right)$ in $\mathcal{V}_m$.

Finally, asymptotic analysis, both types of initial lesion problems, including case of non-inhibited pure bending and case of inhibited pure bending, has weak convergence. Asymptotic analysis revealed that initial lesion is bending-dominated when pure bending is non-inhibited and that initial lesion is membrane-dominated when pure bending is inhibited. Clinically, the primal lesion undergoes transformations under the influence of membrane, bending, and shear tensors. In advanced stages, the transition towards upper bound occurs due to change in coercivity bounds. During the advanced stages of disease, the bending is responsible for introducing progressive disarray of collagen fibers, smooth muscle cells, and ground matrix and thus contributes to rapid progression. Asymptotic analysis suggests that bending strain is relevant for the progression of disease in advanced stages. Hence, asymptotic analysis is a valuable technique for theoretical supplementation to model building and provide insights into the behavior of initial lesion.

6. Concluding remarks

6.1 Conclusion

We constructed the model by using higher-order kinematical assumptions relevant to human cardiovascular system. We called this model the initial lesion model. The weak convergence of the solution to initial lesion model was mathematically substantiated. In the analysis of the initial lesion, we concentrated to seek biological and mathematical insights in order to understand early stages of AD. A general understanding of evolution of initial lesion in aortic dissection is presented. The results presented in this chapter are relevant for the assessment of shell-type lesion in biological systems including human physiology and pathology. At least two observations are to be noted. First, the mathematical analysis of the initial lesion model is distinct from classical shell models. Second, the asymptotic analysis of the initial lesion model is based on degenerating three-dimensional continuum to bending strains to initial lesion behavior. For very thin shells as seen in human vessels' internal lining, the analytical perspective to the initial lesion model given in this chapter can be used in the convergence studies.

6.2 Future scope

Clinically complex situations such as the formation of false lumen either blind or patent in advanced stage of AD merit mathematical analysis perusing coercivity bounds.

Author details

Vishakha Jadaun and Nitin Raja Singh*
Indian Institute of Technology, Delhi, New Delhi, India

*Address all correspondence to: nitinrsingh22@gmail.com

References

[1] Bathe KJ. Finite Element Procedures. 2006

[2] Argyris JH, Kelsey S. Energy Theorems and Structural Analysis. A Generalised Discourse with Applications on Energy Principles of Structural Analysis Including the Effects of Temperature and Non-linear Stress-Strain Relations. London: Butterworths; 1960

[3] Clough RW, Martin HC, Topp LJ, Turner MJ. Stiffness and deflection analysis of complex structures. Journal of the Aeronautical Sciences. 1956;**23**:9

[4] Ahmad S, Irons BM, Zienkiewicz OC. Analysis of thick and thin shell structures by curved finite elements. International Journal for Numerical Methods in Engineering. 1970;**2**(3): 419-451

[5] Reissner E. The effect of transverse shear deformation on the bending of elastic plates. Journal of Applied Mechanics. 1945;**12**:A-69-A-77

[6] Mindlin RD. Influence of rotatory inertia and shear on flexural motions of isotropic, elastic plates. Journal of Applied Mechanics. 1951;**18**:31-38

[7] Badger S et al. Endovascular treatment for ruptured abdominal aortic aneurysm. Cochrane Database of Systematic Reviews. 2017;**5**

[8] Zankl AR et al. Pathology, natural history and treatment of abdominal aortic aneurysms. Clinical Research in Cardiology. 2007;**96**(3):140-151

[9] Legarreta JH et al. Hybrid decision support system for endovascular aortic aneurysm repair follow-up. In: International Conference on Hybrid Artificial Intelligence Systems. Berlin, Heidelberg: Springer; 2010. pp. 500-507

[10] Sakalihasan N, Limet R, Defawe OD. Abdominal aortic aneurysm. The Lancet. 2005;**365**(9470): 1577-1589